Heliyon 10 (2024) e37864

Contents lists available at ScienceDirect

Heliyon

journal homepage: www.cell.com/heliyon

Research article

The prebiotic impacts of galactose side-chain of tamarind xyloglucan oligosaccharides on gut microbiota

Yubo Zhou [a,1], Shuo Tang [b,1], Ying Lv [a], Daihui Zhang [c], Xiaode Huang [b], Yanan Chen [a,**], Chenhuan Lai [a,*], Qiang Yong [a]

[a] Jiangsu Co-Innovation Center of Efficient Processing and Utilisation of Forest Resources, College of Chemical Engineering, Nanjing Forestry University, Nanjing, 210037, PR China
[b] Nanjing Institute of Comprehensive Utilization of Wild Plants, Nanjing, 211111, PR China
[c] Institute of Chemical Industry of Forest Products, Chinese Academy of Forestry, Nanjing, 210042, PR China

ARTICLE INFO

Keywords:
Tamarind xyloglucan
Oligosaccharide
Galactose side-chain
Prebiotic activity
Gut microbiota

ABSTRACT

To explore the impacts of galactose side-chain on the prebiotic activity of xyloglucan oligosaccharides (XGOS), XGOS and de-galactosylated XGOS (DG-XGOS) were prepared from tamarind using an enzymatic method. The differences in structural features of XGOS and DG-XGOS were systematically analyzed. Their *in vitro* fermentation characteristics of human fecal microbiota were explored. These results indicated that both XGOS and DG-XGOS promoted short-chain fatty acids (SCFAs) production, decreased pH, and changed the microbiota composition of the fermentation broth. Comparatively, DG-XGOS was more effective than XGOS in producing SCFAs, inhibiting the phylum Proteobacteria prevalence, and promoting the phyla Bacteroidetes and Actinobacteria prevalence. In summary, the xyloglucan degradation products exert potential prebiotic activity. Removing the galactose side-chains further enhances oligosaccharide utilization by fecal microbiota, offering a valuable approach to improve the biological efficacy of oligosaccharides.

1. Introduction

The human gut microbiota is a highly diverse community of microorganisms that forms a complex ecological system that interacts with the host and environmental factors. Due to its contribution to human health, gut microbiota has been attracted increasing attention recently [1]. Gut microbiome disturbance may increase intestinal permeability, impair the digestion and metabolism capacity, and induce immune responses, thereby potentially inducing various diseases [2]. Several factors affecting gut microbiome include diet, age, host genetic, exercise, and others. Diet plays the most significant role in shaping the gut microbiome [3]. Dietary fiber, as one of the functional foods, is not affected by digestive enzymes, and arrives in the cecum at last [4]. In addition, dietary fiber can be degraded by the microbiota and converted into SCFAs, which can effectively regulate the pH in the large intestine, promote the growth of salutary bacteria, and regulate the structure of gut flora [5]. Therefore, dietary fiber intervention is a crucial strategy to maintain intestinal health by regulating gut microbiota.

* Corresponding author.
** Corresponding author.
E-mail addresses: chenyn18@njfu.edu.cn (Y. Chen), lch2014@njfu.edu.cn (C. Lai).
[1] Yubo Zhou, and Shuo Tang contributed equally to this work, regarding as the first author.

https://doi.org/10.1016/j.heliyon.2024.e37864
Received 17 March 2024; Received in revised form 9 September 2024; Accepted 11 September 2024
Available online 12 September 2024

Plants are one of the most important sources of dietary fiber, including functional polysaccharides and oligosaccharides [6]. Xyloglucan (XG) is a type of hemicellulose found in the cell walls of higher plants. The main chain of XG comprises glucose linked by β-1,4-glycosidic bonds, and some of the glucose residues frequently bear side-chains at O-6 [7]. And the glycosyl residue composition of XG side-chains exhibits diversity due to differences in plants, tissues, and cell types [8]. XG is classified and named based on its side-chain structure to simplify the description of side-chains. G represents the unsubstituted glucose residue in the main chain, whereas what is replaced by a xylose residue at O-6 is defined as X. L and F are respectively used to represent the structures replaced by galactose residues and fucose residues at O-2 position of the xylose residue [9]. The repeating structure units of XG have been investigated by endoglucanase hydrolysis. Tamarind XG is mainly consist of repeating oligosaccharides structure such as XXXG, XLXG, XXLG, and XLLG.

Currently, in commercial production, XG is mainly obtained from tamarind seeds, a leguminous dicotyledonous plant that is widely distributed in Africa and Asia. Given its abundant resources, low price, excellent rheological properties, and excellent gelling properties, XG has been widely applied in food additives, daily packaging films, drug release carriers, and other fields [10]. Recent studies have also proposed that tamarind XG exhibits excellent prebiotic activity, and can also be transformed into a series of SCFAs in the large intestine and other low molecular weight active substances [11,12]. In addition to affecting the composition of the gut community, these secondary metabolites also provide energy and reshape the host immune system [13].

It has been widely accepted that the prebiotic activities of polysaccharides with a high molecular weight are usually limited by their high liquid viscosity and poor solubility [14]. Reducing the molecular weight of dietary fibers by partial hydrolysis can improve biological activity in terms of prebiotic, antioxidant, anti-inflammatory, metabolic syndrome, antibacterial, and anti-tumor activities [15]. *Li* et al. investigated the *in vitro* fermentation of two hydrolyzed XG fractions by human fecal microbiota, which revealed that hydrolyzed XG utilization by microbiota was accelerated with a decreasing molecular weight [14]. Furthermore, it has been observed that tamarind xyloglucan oligosaccharide (XGOS) attenuates metabolic disorders via the gut-liver axis in mice by increasing the gut microbiota diversity [16]. Besides molecular weight, the structure of dietary fiber such as monosaccharide composition, glycosyl side-chain, and glycosidic linkages also influences its prebiotic activity. A previous study has been reported that the presence of arabinose side-chains has a significant impact on the biological activity of arabinogalactose [17]. However, the effects of glycosyl side-chains on XGOS fermentation by the human gut microbiota have rarely been reported. The enzymatic degradation of XG with β-galactosidase has been conducted in the previous studies to investigate the effects of galactose side-chain on the thermoreversible gelation of XG [18,19].

Therefore, to explore the impacts of galactose side-chain on the prebiotic activity of XGOS, XGOSs with different galactose contents were prepared by a step-wise enzymatic hydrolysis with cellulase and β-galactosidase in this study. The structural properties of the two oligosaccharides were compared based on their glycosidic composition and nuclear magnetic resonance (NMR) analyses. More importantly, *in vitro* human fecal microbial fermentation of these two oligosaccharide was conducted and their impacts on SCFAs production, oligosaccharides consumption, and microbiota composition was systematically investigated. This study will help better understand the prebiotic activity of tamarind XGOS and provide a strategy for improving its prebiotic activity by modifying its glycosyl composition.

2. Materials and methods

2.1. Materials and chemicals

Tamarind seed powder was purchased from Wangwang Biotechnology Co., Ltd. (Shanghai, China). The cellulase (UTA-8) from *Trichodermareesei* belonging to the GH45 family was obtained from Hunan Youtell Biochemical., Ltd. (Hunan, China), and had an activity of 59 FPU/g. The β-Galactosidase (EC 3.2.1.23) from *Aspergillus oryzae*, belonging to the GH35 family was obtained from Sigma-Aldrich (Shanghai, China), and its activity was 8 U/mg, monosaccharide standards, and SCFAs standards were purchased from Sigma-Aldrich (Shanghai, China). The other reagents were purchased from Aladdin Chemical Reagent Co., Ltd. (Shanghai, China).

2.2. Preparation of tamarind xyloglucan

XG was extracted from tamarind seed powder using water at 90 °C, pH 4.5, and a solid-to-liquid ratio of 1:40 for 50 min. The pH was adjusted using a citric acid solution. The supernatant was obtained by centrifugation at 8000 rpm for 10 min to remove solid residues. Then, XG was precipitated from the supernatant by adding isopropanol to a final concentration of 50 %. The XG was washed with 50 % isopropanol thrice, followed by freeze-drying.

2.3. Enzymatic preparation of xyloglucan oligosaccharide with different galactose side-chain contents

Prior to prepare oligosaccharides with different galactose contents. XG was treated with β-galactosidase to remove the galactose side-chains, using a modified method reported by Shirakawa et al. [18] In details, enzymatic hydrolysis of XG (20 g/L) was performed with 8 U/mL β-galactosidase at 50 °C, pH 5.0 for 48 h. Samples were withdrawn at 8, 16, 24, and 48 h of enzymatic hydrolysis. Galactose concentrations in the supernatants were determined to monitor the galactose side-chain removal ratio. After hydrolysis, the enzyme was inactivated by boiling the reaction mixture for 10 min. Subsequently, de-galactosylated XG (DG-XG) was precipitated from the supernatant, washed, and freeze-dried as described above.

Then XG and DG-XG were subjected to enzymatic hydrolysis with cellulase to prepare oligosaccharides with different galactose

contents. Enzymatic hydrolysis process was conducted at 50 °C, pH 4.8, and 20 g/L polysaccharide concentration, with an enzyme loading of 0.1 U/mL. After 48 h of hydrolysis, the hydrolysate were obtained by centrifugation and heated in boiling water for 10 min. We performed 200 Da dialysis of the enzymatic hydrolysate for 48 h. Then the supernatants were subjected to solvent precipitation using 50 % isopropanol. The oligosaccharides were separated from the mixture, and remained in the residual supernatants. The oligosaccharides prepared from XG and DG-XG were designated XGOS and DG-XGOS, respectively.

2.4. Analysis of xyloglucan degradation products content

The quantitative analysis of XGOS and DG-XGOS was performed according to a modified protocol reported by Tao et al. [20] Prior to the quantitative analysis of XGOS and DG-XGOS, the oligosaccharides should be separated from the mixture using solvent precipitation as described above. Then a one-step acid hydrolysis was performed. In brief, oligosaccharide samples were subjected to 4 % (w/w) sulfuric acid at 121 °C for 1 h. After that, the acid hydrolysate was analyzed by a Dionex ICS-5000 system equipped with an CarboPac PA10 column.

2.5. Molecular weight determination and nuclear magnetic resonance analysis

As for molecular weight determination, samples (10 μL) were configured as 2–4 g/L solution and analyzed by a high-performance gel permeation chromatography equipped with three columns in series of Waters Ultrahydrogel ™ 2000, Ultrahydrogel ™ 250, and Ultrahydrogel ™ 120 columns, equipped with a refractive index detector. The number-average (M_n) and weight-average molecular weights (M_w) of the samples were calculated with a Dextran standards calibration curves.

Additionally, two oligosaccharide samples were analyzed with NMR. We added 50 mg of sample and 5 mg of sodium dichloroacetate (DSS, as an internal standard) were added to 450 μL of D_2O as a test sample. The samples were analyzed by ^{1}H NMR, ^{13}C NMR, ^{1}H–^{1}H COSY, ^{1}H–^{1}H TOCSY, ^{1}H-^{13}C HSQC, and ^{1}H-^{13}C HMBC using a Bruker Avance 600 MHz spectrometer in combination with the previous literature [21,22]. The data obtained were analyzed using the Bruker Topspin software.

2.6. MALDI-TOF MS analysis

The XGSO and DG-XGOS were analyzed by MALDI-TOF to confirm the specific structures of the two oligosaccharide samples. Oligosaccharides were dissolved in 2,5-dihydroxybenzoic acid aqueous solution which mixed with equal volume of methanol/water (1:1 v/v) solution. The instrument was operated at an accelerating voltage of 20 kV and data were collected in positive ion mode. A 200 Hz pulsed ND: YAG laser (335 nm) was used for MALDI. Mass spectra were acquired on an Auto III MALDI-TOF (Applied Bruker Daltonics, USA). Spectra were recorded in the mass range *m/z* 600–3000.

2.7. In vitro fecal fermentation of tamarind xyloglucan oligosaccharide

2.7.1. Preparation of growth medium

The growth medium was prepared according to the previous study [23]. Each 1 L of bacterial culture medium contains sodium chloride (0.1 g), potassium dihydrogen phosphate (0.04 g), $CaCl_2{\cdot}6H_2O$ (0.01 g), bile salt (0.5 g), yeast extract (2.0 g), casein peptone (2.0 g), $MgSO_4{\cdot}7H_2O$ (0.01 g), heme (0.02 g), sodium bicarbonate (2.0 g), cysteine HCl (0.5 g), azuron (1.0 mg), vitamin K_1 (10 μL), tween 80 (2.0 mL), and ultra-pure water. The pH was set to 7.0 using 0.2 M hydrochloric acid solution. After preparation, the culture medium was autoclaved at 121 °C for 20 min.

2.7.2. Preparation of fecal slurry and fermentation

Fresh fecal samples were obtained from three healthy young volunteers who had not taken antibiotics or probiotic products within 3 months. The fecal samples were diluted to 10 % (w/v) with sterile normal saline, homogenized in a stomacher, and centrifuged at 500 rpm for 5 min at 4 °C to obtain fecal slurries. Subsequently, 0.5 mL of fecal slurries and 4.5 mL of medium (basal medium, basal medium supplemented with 5 g/L XGOS, or basal medium with 5 g/L DG-XGOS added to the vessels. Fermentation was performed in an anaerobic chamber at 37 °C. After 0, 3, 6, 12, 24 and 48 h of fermentation, 5 mL of each sample was stored in liquid nitrogen immediately. Each group comprised three replicate vessels.

2.7.3. Microbial community analysis

After fermentation, the samples were centrifuged at 8000 rpm for 15 min at 4 °C. The precipitates were washed with phosphate buffer saline (PBS) solution, and the total bacterial deoxyribonucleic acid (DNA) was extracted using a bead-beating and phenol-chloroform method [24]. The quality of the DNA samples was assessed by gel electrophoresis, and their concentrations and purity were determined to use a NanoDrop 2000 spectrophotometer (Thermo Fisher Scientific, Waltham, USA). The PCR amplification of the V3-V4 region of the bacterial 16S rRNA gene was performed as previously reported [25]. Then the amplicon were extracted from agarose gels, purified by the AxyPrep DNA gel extraction kit, and a QuantiFluor™-ST fluorometer was used for quantitative analysis. The purified amplicon were pooled in equimolar amounts and paired-end sequenced using an Illumina MiSeq platform (San Diego, USA) [26].

The raw FASTQ files were demultiplexed and quality-filtered using the QIIME software. The operational taxonomic units (OTUs) were clustered with a threshold of 97 % identity using the UPARSE software, and the chimeric sequences were identified and removed

using the UCHIME software. The phylogenetic affiliation of each 16 S rRNA gene sequence was analyzed using the RDP Classifier.[19] Rarefaction analysis, species accumulation curves, alpha diversity, beta diversity, and linear discriminant analysis effect size (LEfSe) analyses were conducted using the MOTHUR software (version 1.29.0). The statistical significance of the differences in bacterial composition among the different groups was assessed using the Kruskal-Wallis rank sum test [27]. The Tax4Fun package in R was used to predict the microbial function. The abundance predictions of Kyoto Encyclopedia of Genes and Genomes (KEGG) orthologs and KEGG pathways of the bacterial communities were calculated based on the SILVA123 databases.

2.8. SCFAs analysis of tamarind xyloglucan during in vitro fecal fermentation

The fermentation broth was centrifuged at 10,000 rpm for 10 min at 4 °C and filtrated by a 0.22 μm filter unit. Then, the SCFAs content of each sample was determined using an Agilent HPLC 1260 instrument with an Aminex HPX-87H column (Bio-Rad Lab, USA). The column temperature was set at 55 °C. The mobile phase was comprised 5 mmol/L sulfuric acid. The flow rate was 0.6 mL/min. The injection volume was 10 μL.

2.9. Statistical analysis

Data are expressed as mean ± standard deviation. Statistical differences among groups were analyzed using one-way analysis of variance (ANOVA) with a post-hoc Duncan's multiple range test using the Origin software (version 2018). $P < 0.05$ is statistically significant.

3. Results and discussion

3.1. Enzymatic preparation of xyloglucan oligosaccharides with two different galactose contents

In order to explore the impacts of the galactose side-chain on the prebiotic activity of XGOS, DG-XGOS with lower galactose contents was prepared by the stepwise enzymatic hydrolysis of native XG. Specifically, the degalactosylation of native XG was performed by enzymatic hydrolysis with β-galactosidase. Fig. 1a shows that the galactose removal ratio increased gradually with the hydrolysis proceeded. A 42.9 % galactose removal ratio was achieved after 48 h, indicating that nearly half of the galactose side-chains were removed from the native XG. A similar observation has been reported in Han's study that β-galactosidase hydrolysis successfully removed 43.1 % of the galactosyl side-chain from XG [28].

Additionally, the enzymatic hydrolysis of XG and DG-XG with cellulase was conducted to prepare the oligosaccharides with different galactose contents. Fig. 1b showed that as the galactose side-chain removal rate increased, the oligosaccharide yield significantly decreased. Specifically, the cellulase enzymatic hydrolysis of native XG achieved the highest oligosaccharide yield (73.6 %). As expected, nearly no monosaccharide was released during cellulase hydrolysis (data not shown), indicating that the directional preparation of XGOS was achieved using commercial cellulase [7,29]. When the DG-XG, with a galactosyl removal rate of 14.0 %, was used as the hydrolysis substrate, the oligosaccharide yield decreased to 52.9 %. As the galactosyl removal rates of XG increased to 36.2 and 42.8 %, the oligosaccharide yields further decreased to 46.1 % and 40.8 %, respectively. With the removal of the galactose side-chain, the polysaccharide chains gradually aggregated into a spherical shape, and the solubility is greatly reduced. These results indicated that the removal of galactose side-chain enabled XG to form thermoreversible gel, and significantly reduced the solubility of long-chain polysaccharides and increased their viscosity, providing a possible explanation for why the enzymatic hydrolysis yield of DG-XG was lower than that of native XG with a higher galactose side-chain [12,18].

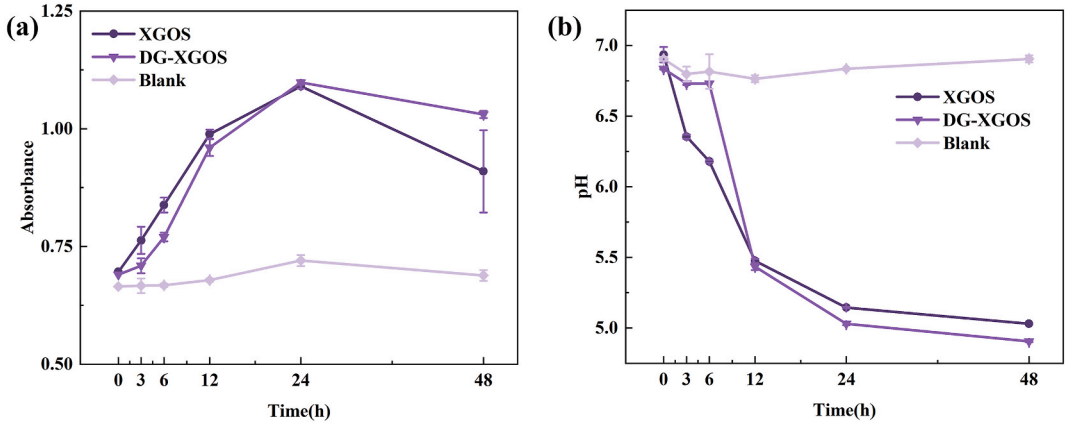

Fig. 1. Step-wise enzymatic tamarind xyloglucan hydrolysis. (a) Removal rate of galactose side-chain during β-galactosidase hydrolysis; (b) Effects of galactose side-chain removal on enzymatic preparation of oligosaccharides using cellulase.

3.2. Structural features of XGOS and DG-XGOS

3.2.1. Glycosyl composition and GPC analysis

The molecular weight and glycosyl composition of XG with and without stepwise enzymatic hydrolysis are shown in Table 1. An obvious change on molecular weight was observed, particularly for the degradation products after cellulase hydrolysis. It is clear that cellulase is effective at degrading the chains, and highly polymerized XG and DG-XG can be degraded into oligosaccharides with very low polymerization. Cellulase is a complex enzyme consisting mainly of exoglucanase, endoglucanase, and β-glucosidase. The main chain of XG is first degraded by endoglucanase into short chains consisting of 7–9 glycosyl groups, and the xylosyl and galactosyl groups on these short chains are subsequently removed by α-xylanase and β-galactosidase [30], which is consistent with our findings that the average degree of polymerization (DP) of XGOS and DG-XGOS was 8 and 6 respectively (Table 1).

Simultaneously, our study found that the molar ratio of DG-XG to DG-XGOS modified by β-galactosidase was significantly different from the original, which was Glu: Gal = 1.00:0.17, verified that the hydrolysis of β-galactosidase successfully removed half of the galactose group. However, the monosaccharide molar ratio of XG to XGOS in the monosaccharide component was similar to that of Glu: Gal (1.00:0.38). The molar ratio of the side-chain-removed polysaccharides and oligosaccharides were similar, indicating that the degradation of xyloglucan by cellulase did not affect its glycosyl composition. Han's study also used β-galactosidase for side-chain degradation of XG with galactosyl removal of 33.3, 38.9, 41.5, and 43.1 % at 8, 16, 32, and 48 h, respectively, which is more or less the same as the present study [28].

3.2.2. NMR analysis of xyloglucan oligosaccharide

The chemical shifts of the various functional groups of the tamarind oligosaccharides are listed in Table 2. The ^{1}H NMR and ^{13}C NMR spectra signals of XGOS were crowded in a narrow region within 3.00–5.3 ppm and 60–105 ppm respectively, which were characteristic peaks of typical polysaccharides. Taking XGOS as an example, the peak at δ 4.70 ppm in the ^{1}H NMR spectrum was attributed to the Hydrogen-deuterium oxide (HDO) (Fig. 2a) [31]. In the analysis of ^{1}H NMR spectra, compared to XGOS (Fig. 2a), the signal intensity of G-H1 (5.16 ppm) was reduced in the ^{1}H spectrum of DG-XGOS (Fig. 3a). Correspondingly, the signal intensities of D-C1 and D-C2 (105.19 ppm) were also lower in the ^{13}C spectrum of DG-XGOS (Fig. 3b) than in that of the XGOS group. On the contrary, the intensity of the C-H1 (4.51 ppm) peaks in the ^{1}H spectrum of DG-XGOS increased, indicating a significant reduction in the number of galactose groups. In the analysis of HMBC spectra (Fig. S1d), the presence of Gal-(1,2)-Xyl in the side-chain structure was indicated by the transitions from G-H2 (3.36 ppm) to D-C1 (104.42 ppm). A clear cross peak between B-H1 (4.55 ppm) and A-C4 (80.09 ppm) was observed, which also confirms that the main chain structure is β-(1,4)-D-glucan composition [32].

3.2.3. MALDI-TOF MS analysis of xyloglucan oligosaccharide

MALDI-TOF MS was used to determine the specific composition of XGOS and DG-XGOS oligosaccharides. As shown in Fig. 4a, when the seed powder of Tamarind was degraded by cellulase, the polysaccharide long chain was cleaved into low molecular weight repeating units, such as oligosaccharide products of XLLG (1409), XXLG/XLXG (1247), XXXG (1085), and GXXG (953). Among them, XLLG which contains two galactose glycosyls has the highest proportion, followed by XXLG/XLXG contains only one galactose glycosyl while XXXG and GXXG without galactose glycosyl has lower content. In addition, there are also oligosaccharide characteristic peaks at 2777, 2615, and 2453 (*m/z*), whose repeating units are 7 glucose in main chains, and 7 xylose are connected to each glucose glycosyls, while galactose is 4, 3, and 2, respectively, connected to xylose glucosyls. This is because the spatial hindrance formed by the xylose and galactose groups on the side-chains prevents further degradation of the main chains of these repeating units.

The oligosaccharide components degraded by β-galactosidase showed significant changes, as shown in Fig. 4b, which represents a decrease in the signal peak of XLLG and a significant increase in the characteristic peaks of XLXG/XXLG, XXXG, and GXXG compared to XGOS. This proves that the proportion of components of oligosaccharides prepared by β-galactosidase has significantly decreased. And subsequently, these oligosaccharide components will be used in *vitro* fermentation.

Tuomivaara et al. investigated the process flow of enzymatic degradation and xylose side-chain removal of tamarind polysaccharide, and investigated its oligosaccharide components. Similar to our results, the basic repeating units obtained after endoglucanase degradation of the main chain were XLLG, XXLG, XXXG [7].

3.3. Changes in short chain fatty acids production during in vitro fermentation

The prebiotic activity is one of the most significant features of functional oligosaccharides. We compared the prebiotic activities of XGOS and DG-XGOS by analyzing the production of SCFAs. Increasing evidence suggests that oligosaccharides exert a significant

Table 1
Glycosyl composition and molecular weight of XG, XGOS, DG-XG and DG-XGOS.

Sample	Molecular weight			Glycosyl composition
	M_n (kDa)	M_w (kDa)	DP	Glu:Gal:Xyl
XG	3281.50	3292.30	18290	1.00: 0.38: 0.61
XGOS	1.36	1.44	8	1.00: 0.37: 0.61
DG-XG	257.03	261.72	1480	1.00: 0.17: 0.58
DG-XGOS	1.08	1.18	6	1.00: 0.16: 0.60

Table 2
^{1}H and ^{13}C chemical shift assignments of xyloglucan oligosaccharides.

Sugar Residue	H1/C1	H2/C2	H3/C3	H4/C4	H5/C5	H6/C6
→4)-β-D-Glcp-(1→ A	4.55/104.63	3.38/72.67	3.65/73.98	3.66/80.09	3.50/75.06	3.96 (3.82)/59.82
→4,6)-β-D-Glcp-(1→ B	4.55/104.61	3.38/72.67	3.65/73.98	3.66/80.09	3.50/75.06	3.99 (3.68)/68.01
T-β-D-Glcp-(1→ C	4.51/107.23	3.04/73.42	3.31/73.44	3.12/70.17	3.15/76.22	3.71 (3.53)/60.97
T-β-D-Galp-(1→ D	4.56/105.19	3.61/70.09	3.90/72.56	3.69/69.41	3.72/78.68	3.78 (3.32)/61.13
→4)-β-D-Galp-(1→ E	4.56/105.19	3.61/70.09	3.90/72.56	3.64/73.91	3.72/78.68	3.78 (3.32)/61.13
T-α-D-Xylp-(1→ F	4.95/101.26	3.53/71.43	3.71/73.25	3.91/68.54	3.76 (3.56)/61.51	
→2)-α-D-Xylp-(1→ G	5.16/101.36	3.65/74.76	3.89/71.90	3.67/71.00	3.76 (3.35)/63.98	
→4)-α-D-Xyl H	5.18/94.45	3.56/72.27	3.65/71.86	3.75/77.45	3.76 (3.83)/59.89	

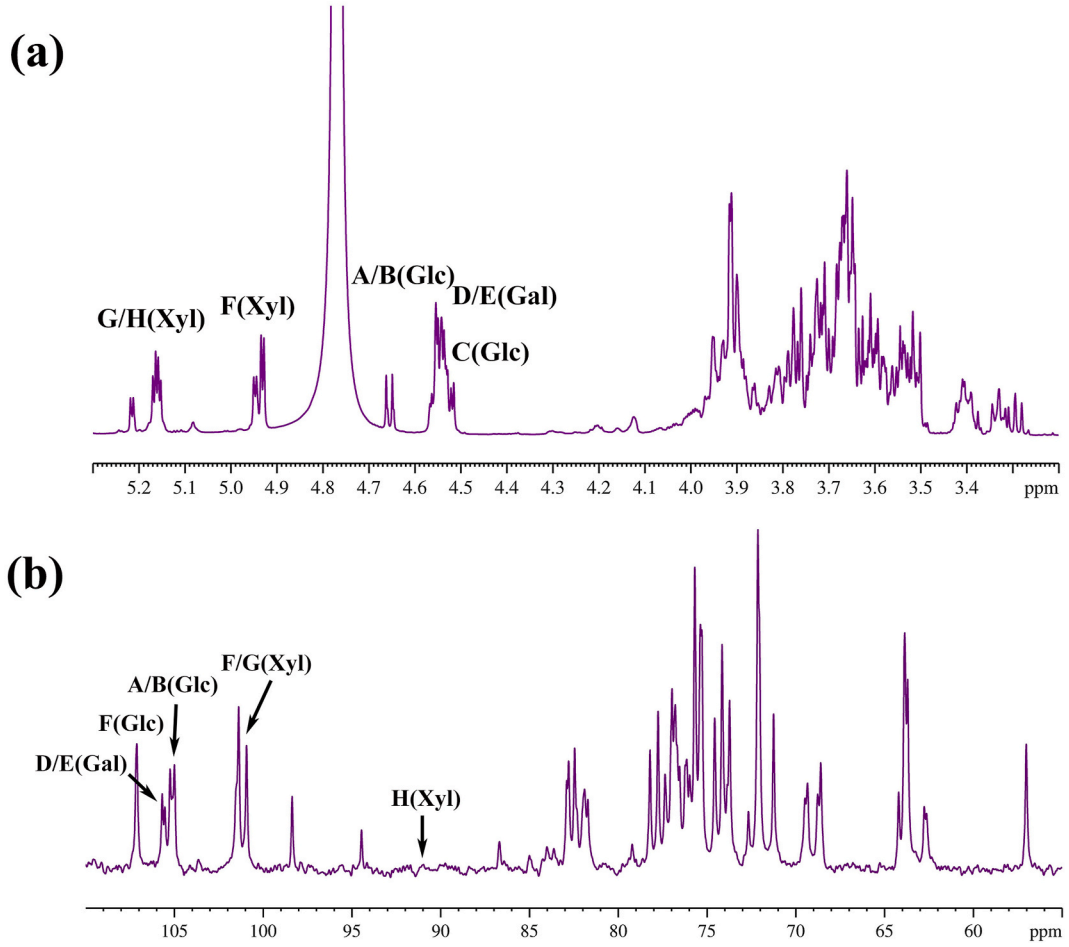

Fig. 2. The structural characterization of XGOS was determined using (a) ^{1}H NMR spectrum; (b) ^{13}C NMR spectrum.

impact on SCFA production in the human gut. The regulation of SCFAs can change people's emotions and cognition by affecting their metabolic function, immune regulation, and secretion system, which is considered a potential therapeutic target for depression [33]. Alterations in SCFAs also increase insulin levels by activating free fatty acid receptors GPR41/43 and GPR109A, thereby achieving a hypoglycemic effect [34].

In this study, we measured the levels of acetic acid, propionic acid, and butyric acid to determine the changes in SCFAs levels mediated by XGOS and DG-XGOS during fermentation. The results suggested that both XGOS and DG-XGOS rapidly increased the levels of acetic acid, propionic acid, and total SCFAs whereas the butyric acid level was closer to a straight line (Table 3). After 3 h of fermentation, the two oligosaccharides produced significantly more SCFAs than the control group. Within 12 h, the two oligosaccharides produced similar levels of SCFAs. However, after 12 h, their abilities diverged, though both eventually leveled off. This is reflected in the fact that, except for the higher production of propionic acid in XGOS than in DG-XGOS, the production levels of other SCFAs and total acids were lower in XGOS group (1.3293 g/L) and DG-XGOS group (1.4742 g/L) was significantly higher than that of

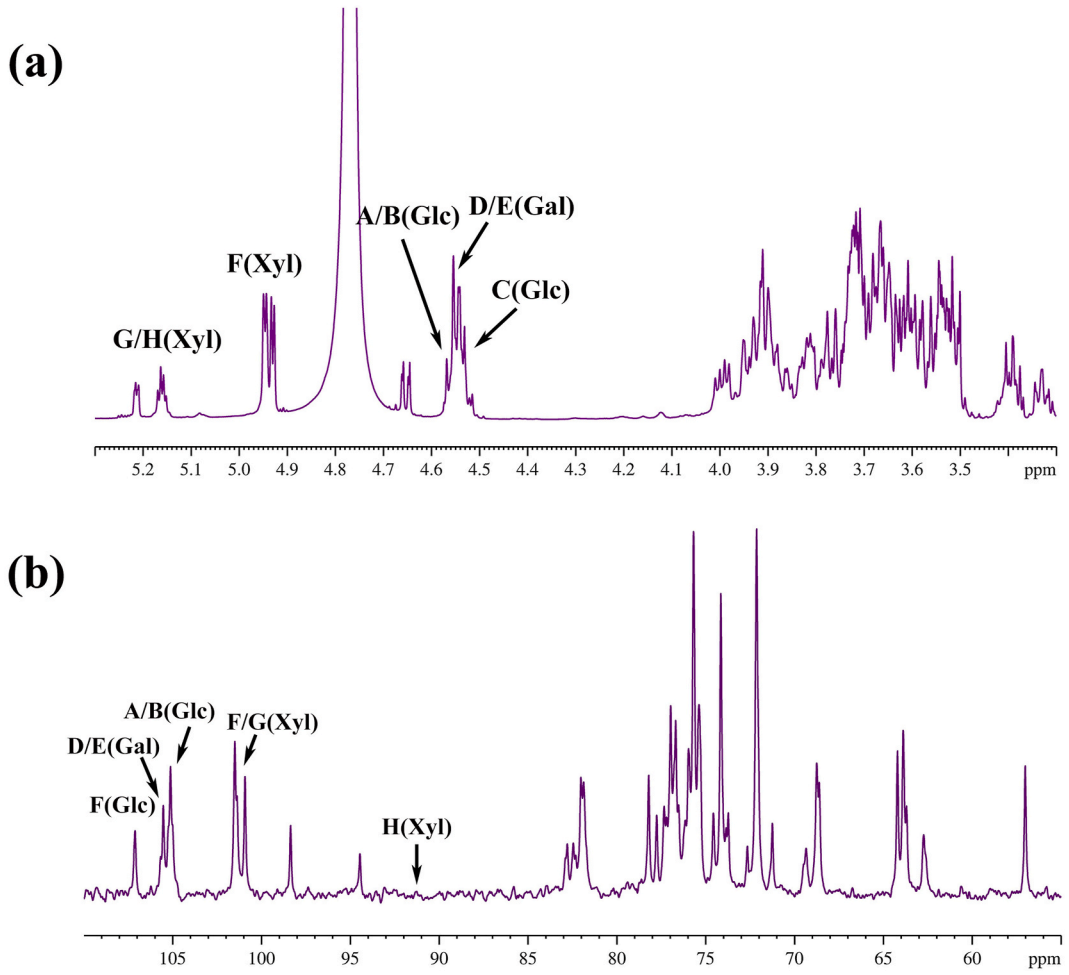

Fig. 3. The structural characterization of DG-XGOS was determined using (a) ^{1}H NMR spectrum; (b) ^{13}C NMR spectrum.

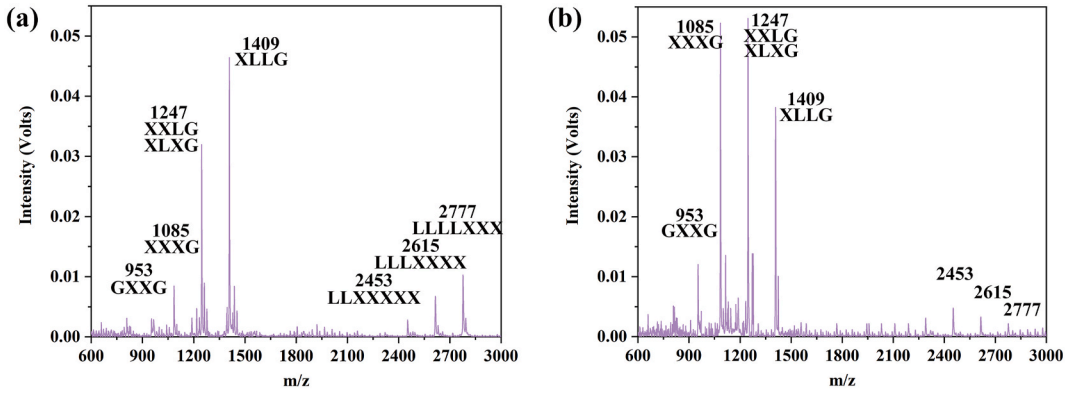

Fig. 4. MALDI-TOF MS analysis of (a) XGOS and (b) DG-XGOS

the control group (0.4625 g/L) (Table 3). At the same time, on analyzing the molar ratio of three acids (acetic acid, propionic acid, and butyric acid), it was found that the molar ratio of the three acids in the XGOS group increased from 1.00:0.36:0.15 at 0 h to 1.00:0.27:0.26 at 48 h, while the molar ratio of the three acids in the DG-XGOS group increased from 1:0.36:0.17 at 0 h to 1:0.25:0.40 at 48 h. Acetic acid and propionic acid contents were higher than that of butyric acid in the early fermentation stage, while the molar ratio of the two components of butyric acid to propionic acid in the total SCFAs were significantly increased throughout the entire

Table 3
Concentration of short-chain fatty acids *in vitro* fermentation broth after 0, 3, 6, 12, 24, and 48 h incubation.

Item		XGOS	DG-XGOS	Blank	*P* values
0 h	Acetic acid (g/L)	0.1760 ± 0.0017	0.1488 ± 0.0031	0.1187 ± 0.0013	–
	Propionic acid (g/L)	0.0632 ± 0.0043	0.0538 ± 0.0021	0.0467 ± 0.0012	–
	Butyric acid (g/L)	0.0273 ± 0.0003	0.0255 ± 0.0065	0.0221 ± 0.0031	–
	Total SCFAs (g/L)	0.2664 ± 0.0014	0.2281 ± 0.0002	0.1876 ± 0.0002	–
3 h	Acetic acid (g/L)	0.3537 ± 0.0033^{a}	0.3214 ± 0.0033^{b}	0.2048 ± 0.0010^{c}	<0.001
	Propionic acid (g/L)	0.0957 ± 0.0016^{a}	0.0843 ± 0.0031^{a}	0.0578 ± 0.0001^{b}	0.002
	Butyric acid (g/L)	0.0610 ± 0.0039^{a}	0.0528 ± 0.0006^{ab}	0.0415 ± 0.0009^{b}	0.023
	Total SCFAs (g/L)	0.5104 ± 0.0022^{a}	0.4585 ± 0.0070^{b}	0.3041 ± 0.0020^{c}	<0.001
6 h	Acetic acid (g/L)	0.5071 ± 0.0004^{a}	0.5043 ± 0.0032^{a}	0.2358 ± 0.0032^{b}	<0.001
	Propionic acid (g/L)	0.1373 ± 0.0020^{a}	0.1292 ± 0.0002^{a}	0.0691 ± 0.0022^{b}	<0.001
	Butyric acid (g/L)	0.0890 ± 0.0005^{a}	0.0886 ± 0.0009^{a}	0.0614 ± 0.0006^{b}	<0.001
	Total SCFAs (g/L)	0.7334 ± 0.0021^{a}	0.7221 ± 0.0022^{a}	0.3445 ± 0.0060^{b}	<0.001
12 h	Acetic acid (g/L)	0.6885 ± 0.0025^{a}	0.6625 ± 0.0033^{b}	0.2665 ± 0.0005^{c}	<0.001
	Propionic acid (g/L)	0.1960 ± 0.0005^{a}	0.1990 ± 0.0003^{a}	0.0794 ± 0.0016^{b}	<0.001
	Butyric acid (g/L)	0.1504 ± 0.0034^{a}	0.1244 ± 0.0063^{b}	0.0685 ± 0.0016^{c}	0.002
	Total SCFAs (g/L)	1.0349 ± 0.0054^{a}	0.9859 ± 0.0093^{b}	0.3876 ± 0.0038^{c}	<0.001
24 h	Acetic acid (g/L)	0.8056 ± 0.0005^{b}	0.8367 ± 0.0020^{a}	0.2573 ± 0.0034^{c}	<0.001
	Propionic acid (g/L)	0.2339 ± 0.0005^{a}	0.2212 ± 0.0033^{b}	0.0899 ± 0.0013^{c}	<0.001
	Butyric acid (g/L)	0.1826 ± 0.0003^{b}	0.3004 ± 0.0001^{a}	0.0949 ± 0.0107^{c}	<0.001
	Total SCFAs (g/L)	1.2221 ± 0.0002^{b}	1.3583 ± 0.0012^{a}	0.4421 ± 0.0060^{c}	<0.001
48 h	Acetic acid (g/L)	0.8667 ± 0.0059^{b}	0.8974 ± 0.0021^{a}	0.2684 ± 0.0002^{c}	<0.001
	Propionic acid (g/L)	0.2378 ± 0.0048^{a}	0.2199 ± 0.0039^{a}	0.1013 ± 0.0016^{b}	<0.001
	Butyric acid (g/L)	0.2248 ± 0.0014^{b}	0.3569 ± 0.0026^{a}	0.0929 ± 0.0009^{c}	<0.001
	Total SCFAs (g/L)	1.3293 ± 0.0093^{b}	1.4742 ± 0.0085^{a}	0.4625 ± 0.0005^{c}	<0.001

Data are expressed as mean ± standard deviation. Blank, negative control (no additional carbohydrate); XGOS, xyloglucan oligosaccharide; DG-XGOS, de-galactosylated oligosaccharide. Different superscript letters in the same row indicate significant differences between the groups ($P < 0.05$, n = 3).

fermentation process. This indicated that the two functional oligosaccharides from tamarind are more likely to produce butyric and propionic acids in the human gut, which was consistent with the results reported by Li et al. [35]This may indicate that XG and its modified polysaccharides mainly regulates the human gut environment through propionic acid and butyric acid. Koh et al. demonstrated that propionic and butyric acids, which are considered to be the main metabolic substrates during gut gluconeogenesis, are effective in establishing a direct link between SCFAs and human metabolism [36].

Large amounts of SCFAs are produced through fermentation and metabolism by bacterial communities in the human gut. This reaction is completed through the glycolytic pathway by bacterial communities such as Bacteroides, Bifidobacterium, Streptococcus, and Lactobacillus. While acetic, propionic, butyric acids are the main products. Among them, acetic acid can be generated by bacterial communities such as Firmicutes through the acetyl CoA or Wood Ljungdahl pathways [37]. Propionic acid is generated in the succinate fermentation pathway, the propylene glycol fermentation pathway, and the acrylate pathway, the strains involved are mainly Bacteroidetes, Ruminalococcus, and Trichosporonaceae, respectively [38]. Butyric acid is mainly obtained by the enzymatic degradation of butyl coenzyme A by Bacteroides and Clostridium [39]. SCFAs are utilized and metabolized by the host as signaling molecules, not only by altering histone acetylation as an important regulator of the epigenome but also by regulating systemic energy homeostasis, which is the main mechanism of soluble polysaccharides mediated human metabolism [40,41]. Therefore, two oligosaccharides of

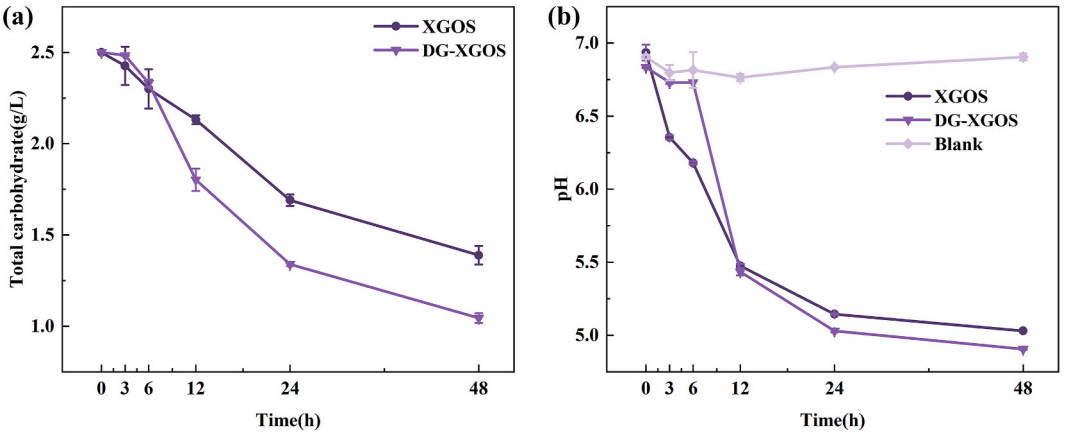

Fig. 5. (a) Total carbohydrate concentration and (b) pH value during XGOS and DG-XGOS fermentation. Blank, negative control (no additional carbohydrate); XGOS, xyloglucan oligosaccharide; DG-XGOS, de-galactosylated oligosaccharide.

tamarind can be absorbed by intestinal microorganisms and produce corresponding benefits to the body through a series of glycolytic reactions, for example, the Wood–Ljungdahl pathway involving acetic acid may couple with the reduction of hydrogen and iron redox proteins, thereby further providing electrons for reducing CO2 to CO; propionic acid, on the other hand, participates in the tricarboxylic acid cycle by generating succinyl CoA to provide energy for the body; butyric acid can indirectly promote the generation of memory T cells and enhance the body's immunity by promoting the absorption and degradation of bile acids to obtain glutamine [42].

3.4. Oligosaccharide consumption and pH values during in vitro fermentation

In our study, XGOS and DG-XGOS were subjected to *in vitro* fermentation by human fecal flora, which resulted in a significant consumption of oligosaccharide (Fig. 5a) and a reduction in pH level (Fig. 5b), suggesting that these two oligosaccharides could be utilized by human fecal microbiota. Interestingly, human fecal microbiota consumed more DG-XGOS content than XGOS content. The pH value of the DG-XGOS group was also lower than that of the XGOS group. These observations, along with the results of the SCFAs production, indicate that tamarind XGOS with the side-chain removal is more easily utilized by the human fecal microbiota. The amount of butyric acid produced by DG-XGOS was significantly higher than that produced by other groups, resulting in lower pH levels. The removal of side-chains became a key factor affecting pH levels and butyric acid generation. One possible reason is that the galactose on the xyloglucan side-chains is oxidized to galacturonic acid during fermentation, The presence of galacturonic acid leads to a lower production butyric acid in the intestine compared to other components [43,44].

Changes in total carbohydrate and pH levels provide a visual representation of how functional oligosaccharides respond to the gut environment. Throughout the entire fermentation process, XGOS was continuously utilized, although there was a slight decrease in utilization after 24 h. The pH level decreased rapidly during the first 12 h and then tended to flatten. However, DG-XGOS consumption was relatively low in the first 3 h but significantly increased from 3 to 24 h, eventually leveling off. This indicates higher fecal microorganisms activity in the early stage of fermentation and a decrease in the later stage, which may be due to the stationary phase of the fecal microbiota [45].

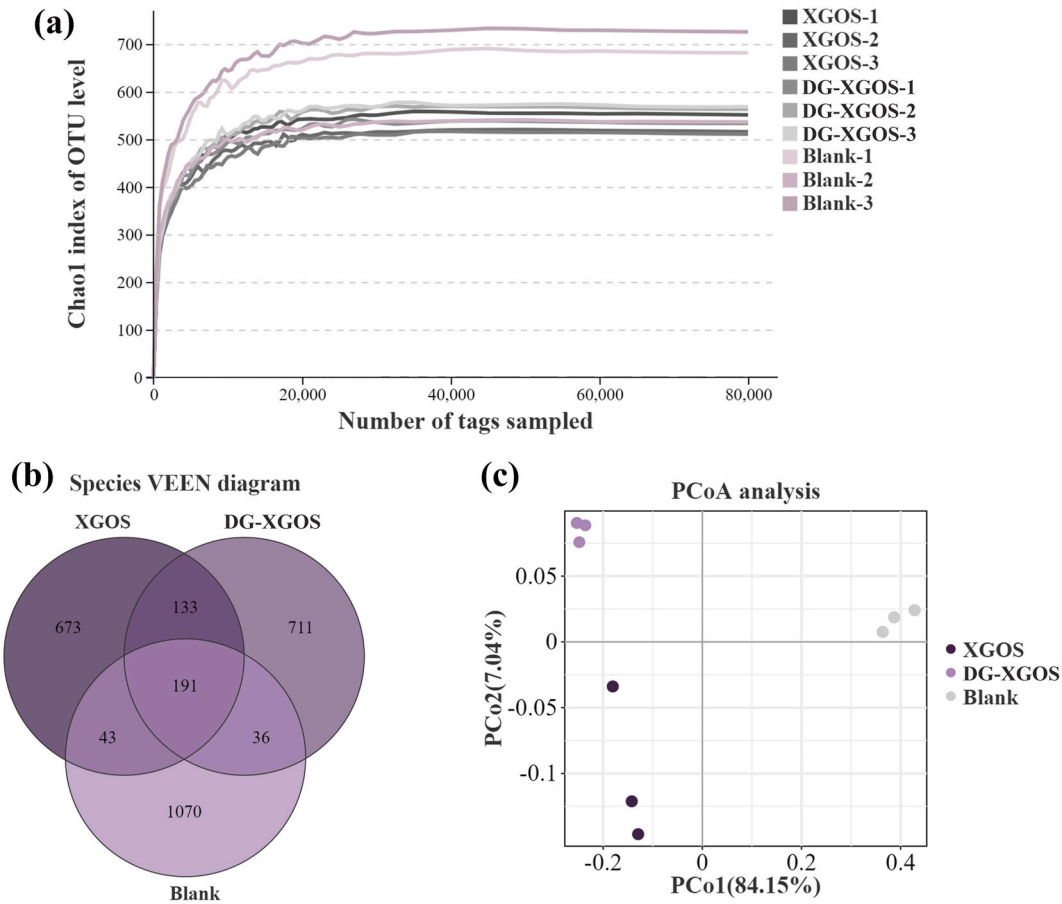

Fig. 6. α Diversity analysis and β Diversity analysis. (a) Chao1 rarefaction curve, (b) Venn diagram and (c) PCoA analysis of human fecal microbiota. Blank, negative control (no additional carbohydrate); XGOS, xyloglucan oligosaccharide; DG-XGOS, de-galactosylated oligosaccharide.

3.5. Diversity and composition of fecal microbiota after in vitro fermentation

The analysis of the V3-V4 region of the 16S rRNA gene through next-generation amplification is a standard method for microbial diversity and composition assessment [46]. In this study, fermentation samples were processed by 16S rRNA gene sequencing to investigate the effects of XGOS and DG-XGOS on the diversity and structure of human fecal microbiota.

The Chao1 rarefaction curve (Fig. 6a) demonstrated that the study achieved high microbial community diversity and sequencing depth. In order to explore the similarity and specificity of the microbial community OTU levels in different habitats, we conducted a Venn diagram analysis of the species richness in the XGOS, DG-XGOS, and Blank groups. A total of 2857 OTUs were identified across the three groups, with 191 being shared OTUs that overlapped (Fig. 6b). In addition, 673, 711, and 1070 unique OTUs were identified in the XGOS, DG-XGOS, and Blank groups, respectively. These findings implied that the addition of oligosaccharides significantly altered the human gut microbial environment.

The calculation of Chao1, ACE, Shannon, and Simpson indices reflects the species diversity and richness of alpha diversity in specific environments. The results suggested that XGOS and DG-XGOS slightly increased the Shannon and Simpson indices, but no significant statistical differences were observed (Table 4). Therefore, the alterations in alpha diversity may not be the key mechanism through which functional oligosaccharides improve gut health. To determine the effects of XGOS and DG-XGOS on the fecal microbiota structure, the beta diversity was assessed using PCoA analysis based on the Bray–Curtis distance. Fig. 6c shows significant clustering characteristics of fecal microbiota composition among the three groups, suggesting that both XGOS and DG-XGOS altered the microbiota composition and that the influence of gut microbial structure caused by DG-XGOS was different from that mediated by XGOS.

To further investigate the changes in the microbiota composition mediated by XGOS and DG-XGOS, the dominant phyla and genera were determined. Our results suggested that Proteobacteria, Firmicutes, Bacteroidetes, and Actinobacteriota were the dominant phyla in the fermentation broth (Fig. 7a). In the Blank group, Proteobacteria accounted for a high proportion, whereas, the addition of the two functional oligosaccharides significantly reduced the abundance of Proteobacteria (Fig. 7b). Proteobacteria contains numerous pathogenic bacteria, and their increase is closely associated with inflammatory bowel disease and metabolic disorders [47]. Hence, the decrease in the abundance of Proteobacteria caused by XGOS and DG-XGOS may reduce the probability of human intestinal diseases. In addition, the relative abundance of Firmicutes (Fig. 7c), Bacteroidetes (Fig. 7d), and Actinobacteriota (Fig. 7e) was increased after treatment with XGOS and DG-XGOS. Studies have demonstrated that Bacteroidetes and Firmicutes improve the gut environment by producing butyric and propionic [48]. Importantly, the genomes of Bacteroidetes and Firmicutes encode carbohydrate active enzymes, outer membrane glycoproteins, and glucose receptors/transporters, all of which constituents orchestrate polysaccharide degradation [13,49]. Actinobacteria, mainly represented by Bifidobacteria, are one of the important probiotics that regulate the immune system and reduce intestinal diseases [50]. Based on these findings, we suspected that XGOS and DG-XGOS improve intestinal health by inhibiting the growth of harmful bacteria, accelerating carbohydrate metabolism, and regulating host immune function.

At the genus level (Fig. 8a), we observed that the relative abundance of *Escherichia-Shigella* belonging to the phylum Proteobacteria was significantly reduced by nearly half in the XGOS (25.69 %) and DG-XGOS (18.07 %) groups compared to the Blank group (41.52 %) (Fig. 8b). The possible mechanism by which this occurred may be attributed to the remarkable increase in *Bifidobacterium* genera observed in this study (Fig. 8e). Evidence has shown that *Bifidobacterium* produces acetic acid, vitamin B, and antioxidants, and consequently protects against the growth of pathogenic microorganisms including *Escherichia-Shigella* [51]. Interestingly, in addition to the upregulation of *Bifidobacteria*, XGOS and DG-XGOS significantly promoted the prevalence of *Phascolarctobacterium* (Fig. 8c), which was in agreement with the prebiotic activity of xylooligosaccharide. Our previous work and other researches have demonstrated that xylooligosaccharide are well-known proliferating factors of *Bifidobacterium* and *Phascolarctobacterium* [52,53]. In this regard, XGOS and DG-XGOS derived from tamarind appear to possess physiological functions similar to those of xylooligosaccharides. Moreover, there was a significant increase in the abundance of *Bacteroides* (Fig. 8d), which is the primary members of *Bacteroidota* phyla. Reports indicate that *Bacteroides* had the strong ability to produce β-glucan digestive enzymes. The removal of galactose side-chains from XG made its structure more similar to β-glucan from oats or barley. This resulted in DG-XGOS promoting *Bacteroides* more obviously like β-glucan [54]. *Bacteroides* is the main genus that produces large quantities of butyric acid *in vivo* [55]. Studies have shown that 20 % of the *Bacteroides* genome is expressed for carbohydrate metabolism, and it also exhibits anti-inflammatory, anti-tumor, and enhancing immune functions in the treatment of gastrointestinal diseases [56,57].

Table 4
Species composition after *in vitro* fermentation broth cultivation α diversity index.

Index	Sobs	Shannon	Simpson	Chao1
XGOS-1	551	4.9705	0.8815	551
XGOS-2	516	4.7675	0.8663	516
XGOS-3	511	4.6504	0.8542	511
DG-XGOS-1	533	5.3093	0.9140	533
DG-XGOS-2	563	5.3100	0.9113	563
DG-XGOS-3	568	5.3650	0.9140	568
Blank-1	681	5.1518	0.8858	681
Blank-2	536	5.0054	0.8567	536
Blank-3	725	5.3501	0.8947	725

Blank, negative control (no additional carbohydrate); XGOS, xyloglucan oligosaccharide; DG-XGOS, de-galactosylated oligosaccharide.

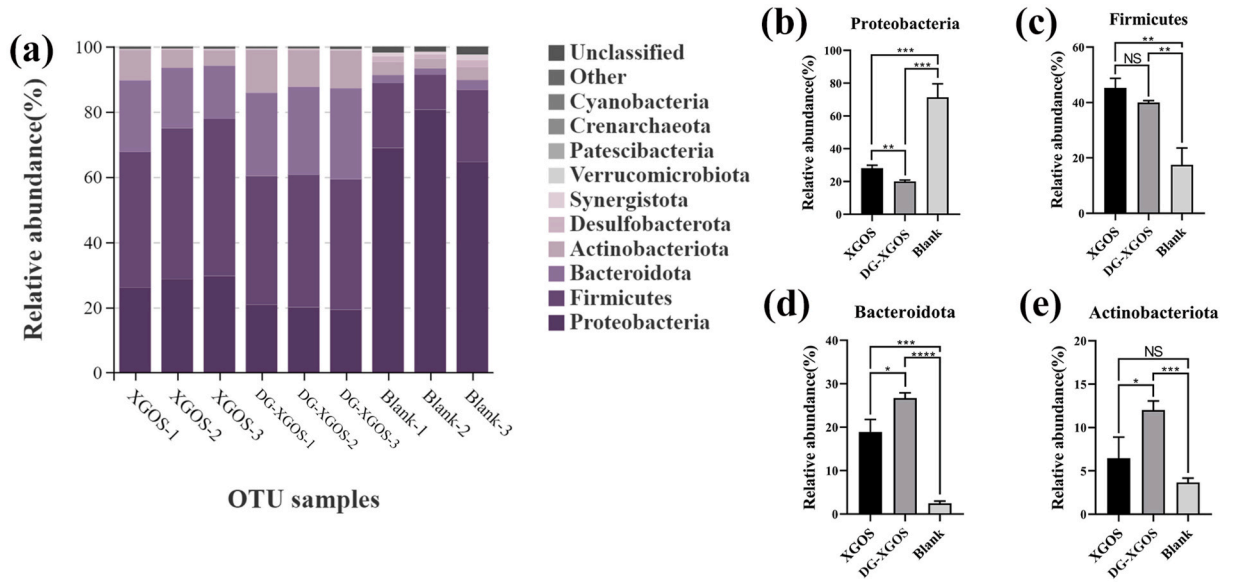

Fig. 7. (a) Bacterial taxonomic profiling at the phylum levels of fermentation broth from different oligosaccharide treatments. The significance difference analysis of the top four dominant bacterial phyla sorted by abundance in the fermentation is as follows: (b) Proteobacteria; (c) Firmicutes; (d) Bacteroidota; (e) Actinobacteriota. Blank, negative control (no additional carbohydrate); XGOS, xyloglucan oligosaccharide; DG-XGOS, de-galactosylated oligosaccharide. Error bars represent standard deviations of three independent experiments. NS, no significant difference; asterisks (*), significant difference ($P < 0.05$); double asterisks (**), highly significant statistical differences ($P < 0.01$); triple asterisks (***), extremely significant statistical differences ($P < 0.001$); Quadruple asterisk (****), extremely significant statistical differences ($P < 0.0001$).

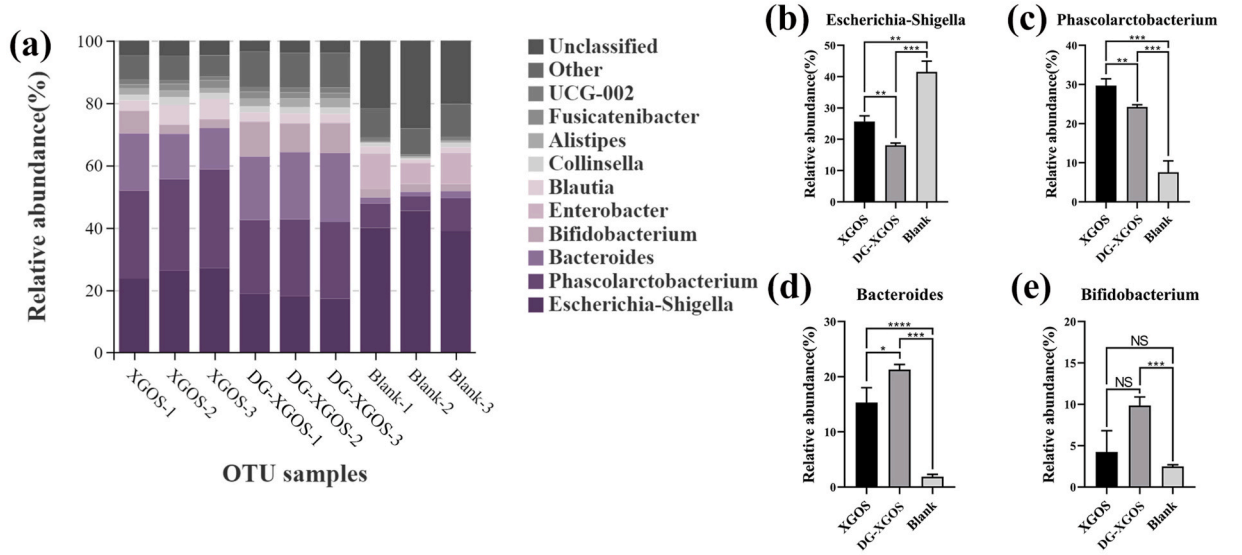

Fig. 8. (a) Bacterial taxonomic profiling at the genus levels of fermentation broth from different oligosaccharide treatments. The significance difference analysis of the top four genera sorted by abundance in the fermentation is as follows: (b) Escherichia-Shigella; (c) Phascolarctobacterium; (d) Bacteroides; (e) Bifidobacterium. Blank, negative control (no additional carbohydrate); XGOS, xyloglucan oligosaccharide; DG-XGOS, de-galactosylated oligosaccharide. Error bars represent standard deviations of three independent experiments. NS, no significant difference; asterisks (*), significant difference ($P < 0.05$); double asterisks (**), highly significant statistical differences ($P < 0.01$); triple asterisks (***), extremely significant statistical differences ($P < 0.001$); Quadruple asterisk (****), extremely significant statistical differences ($P < 0.0001$).

In general, compared to the control group, fermentation changed the diversity of bacterial communities at the phylum level, reduced the abundance of some pathogenic bacteria, and increased the abundance of some beneficial bacteria such as Firmicutes, Bacteroidetes, and Actinobacteria. Among them, Firmicutes occupied a significant position in the XGOS component, while the abundance of Bacteroidetes and Actinobacteria was significantly increased in the DG-XGOS group. Cong et al. found in their study that

the binding site of GII.13/21 in Human noroviruses (huNoVs) can specifically recognize a group of oligosaccharide molecules with a common terminal β-galactose (β-Gal) [58]. This allows oligosaccharide molecules to perform a decoy function [59]. Which can effectively bind oligosaccharides and GII.13/21 in body and prevent NoV associated diseases. There is also a large amount of terminal β-galactose present in xyloglucan. Although currently, no research has proven that the galactose side-chains on the surface of xyloglucan can specifically recognize any pathogen. When relevant research can discover similar functions of wood glucose oligosaccharides, it will greatly pave the way for the research on the biological activity of wood glucose oligosaccharides.

Notably, DG-XGOS exhibited a stronger suppressive effect on the phylum Proteobacteria, particularly the genera *Escherichia-Shigella*, and a greater stimulatory effect on the genera *Phascolarctobacterium* and *Bacteroides*, compared to XGOS. This potentially explains the higher butyric acid production observed with DG-XGOS compared to XGOS [50]. *Phascolarctobacterium* and *Bacteroides* are major producers of butyric acid, and the generation of butyric acid can directly activate the G-protein-coupled-receptor, inhibit histone deacetylases, and serve as energy substrates to inhibit pathogenic bacteria and maintain a balance between co-occurring bacteria and pathogenic bacteria in the intestinal immune system [36,60]. In addition, we examined the differentially abundant species between the XGOS and DG-XGOS groups using LEfSe analysis. The fecal microbiota in the XGOS group was dominated by Firmicutes, whereas in the DG-XGOS group, *Bacteroides* and *Actinobacteriota* were the main components and more beneficial bacteria such as *Bifidobacterium*, *Alistipes*, and *Paraprevotella* were found (Fig. 9a). Moreover, Tax4Fun was used to further reveal the potential metabolic processes mediating the two oligosaccharides. Compared to the Blank group, the XGOS group had significantly higher functional enrichment of environmental adaptation, energy metabolism, and metabolism of cofactors and vitamins, whereas the DG-XGOS group had significantly higher functional enrichment of amino acid metabolism, replication and repair, as well as transcription. Taken together, the galactose branch is a crucial factor affecting the regulation of XGOS in fecal microbiota composition, which may result in discrepancies in SCFAs production and pH changes between XGOS and DG-XGOS (Fig. 9b).

4. Conclusion

In this study, we prepared the debranched oligosaccharide DG-XGOS from tamarind using a stepwise enzymatic hydrolysis method. We then investigated the impact of removing the galactose branch chain on the *in vitro* fermentation characteristics of XGOS. The results showed that both XGOS and DG-XGOS increased the SCFAs production, decreased pH, and inhibited the abundance of some pathogenic bacteria. Meanwhile, DG-XGOS induced changes in the microbiota structure were different from those mediated by XGOS. These observations indicated the activity of tamarind xyloglucan oligosaccharide with the removal of the galactose side-chain is significantly better than that of the original oligosaccharide, which was manifested in the ability to produce more SCFAs, inhibiting the spread of phylum Proteobacteria, and promoting the spread of phyla Bacteroidetes and Actinobacteria.

Ethics statement

The investigations concerning human feces were conducted in accordance with the Code of Ethics of the World Medical Association (Declaration of Helsinki). All procedures were approved by the Animal Welfare and Ethics Committee of Nanjing Forestry University (Permit number: 2024005; Permit time: 4 March 2024). The authors affirm that informed consent was acquired for the experiment on human feces, and assure the perpetual respect of the privacy rights of the human subjects involved.

Funding

This study was supported by the National Natural Science Foundation of China (32201514).

Data availability statement

Data will be made available on request and can be found online.

CRediT authorship contribution statement

Yubo Zhou: Writing – original draft, Investigation. **Shuo Tang:** Writing – review & editing, Visualization. **Ying Lv:** Methodology, Data curation. **Daihui Zhang:** Validation, Methodology. **Xiaode Huang:** Validation, Methodology. **Yanan Chen:** Writing – review & editing. **Chenhuan Lai:** Writing – review & editing, Supervision, Conceptualization. **Qiang Yong:** Validation, Conceptualization.

Declaration of competing interest

The authors declare the following financial interests/personal relationships which may be considered as potential competing interests:Shuo Tang reports financial support was provided by National Natural Science Foundation of China. Co-author (Daihui Zhang) is an associate editor of this journal. If there are other authors, they declare that they have no known competing financial interests or personal relationships that could have appeared to influence the work reported in this paper.

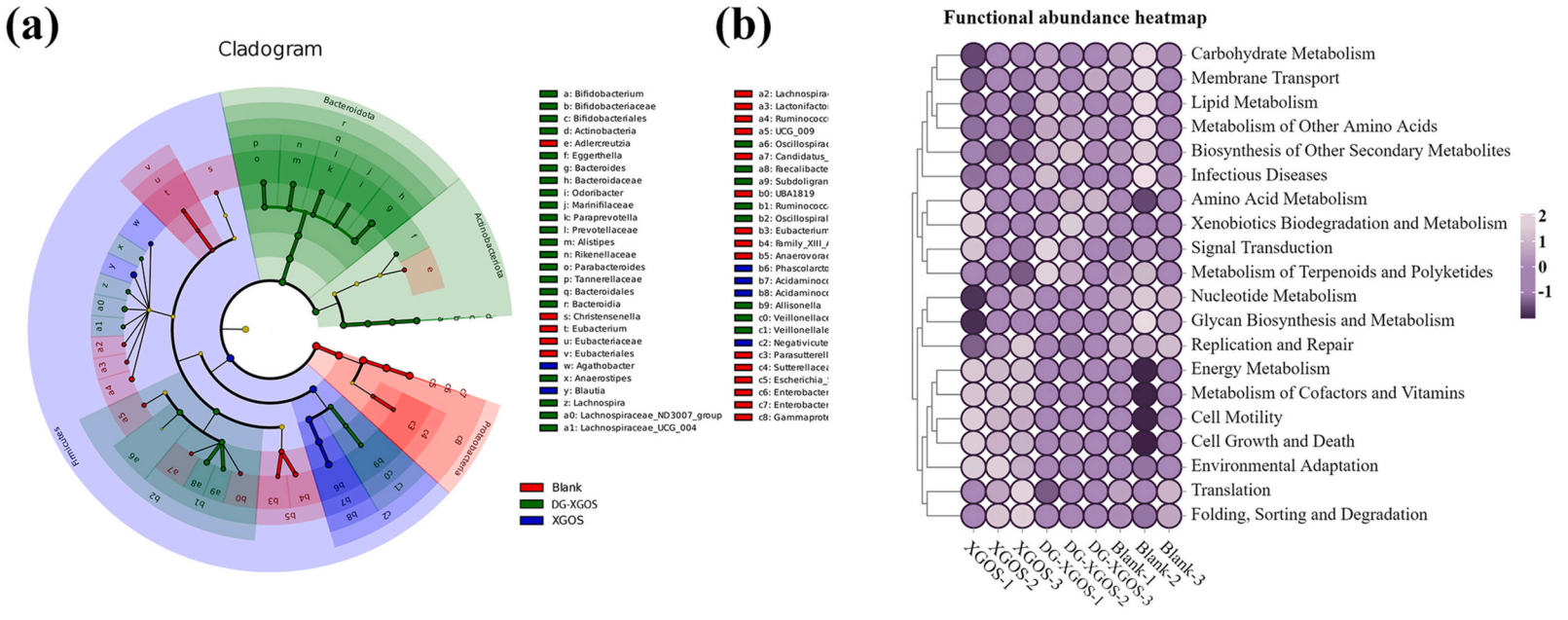

Fig. 9. (a) The taxonomic clado gram obtained from LEfSe analysis of gut microbiota for different treatment groups. (b) Functional heat map of microbial communities. Blank: Negative control (no additional carbohydrate); XGOS: xyloglucan oligosaccharide; DG-XGOS: de-galactosylated oligosaccharide.

Acknowledgements

The authors appreciate the technical assistance provided by Co-Innovation Center of Efficient Processing and utilization of Forest Resources, Nanjing Forestry University.

Appendix A. Supplementary data

Supplementary data to this article can be found online at https://doi.org/10.1016/j.heliyon.2024.e37864.

Abbreviations

XG tamarindus xyloglucan
DG-XG de-galactosylated tamarindus xyloglucan
XGOS oligosaccharides obtained from enzymatic degradation of xyloglucan
DG-XGOS oligosaccharides obtained from enzymatic removal of galactose side-chains and degradation of xyloglucan
SCFAs short-chain fatty acids

References

[1] B. Zhu, X. Wang, L. Li, Human gut microbiome: the second genome of human body, Protein Cell 1 (2010) 718–725, https://doi.org/10.1007/s13238-010-0093-z.
[2] E.Z. Gomaa, Human gut microbiota/microbiome in health and diseases: a review, Antonie Leeuwenhoek 113 (2020) 2019–2040, https://doi.org/10.1007/s10482-020-01474-7.
[3] R.K. Singh, H.-W. Chang, D. Yan, K.M. Lee, D. Ucmak, K. Wong, M. Abrouk, B. Farahnik, M. Nakamura, T.H. Zhu, T. Bhutani, W. Liao, Influence of diet on the gut microbiome and implications for human health, J. Transl. Med. 15 (2017) 73, https://doi.org/10.1186/s12967-017-1175-y.
[4] Q. Xia, Q. Zhao, H. Zhu, Y. Cao, K. Yang, P. Sun, M. Cai, Physicochemical characteristics of Ganoderma lucidum oligosaccharide and its regulatory effect on intestinal flora *in vitro* fermentation, Food Chem. X 15 (2022) 100421, https://doi.org/10.1016/j.fochx.2022.100421.
[5] X. Qiang, C. YongLie, W. QianBing, Health benefit application of functional oligosaccharides, Carbohydr. Polym. 77 (2009) 435–441, https://doi.org/10.1016/j.carbpol.2009.03.016.
[6] W. Qin, L. Sun, M. Miao, G. Zhang, Plant-sourced intrinsic dietary fiber: physical structure and health function, Trends Food Sci. Technol. 118 (2021) 341–355, https://doi.org/10.1016/j.tifs.2021.09.022.
[7] S.T. Tuomivaara, K. Yaoi, M.A. O'Neill, W.S. York, Generation and structural validation of a library of diverse xyloglucan-derived oligosaccharides, including an update on xyloglucan nomenclature, Carbohydr. Res. 402 (2015) 56–66, https://doi.org/10.1016/j.carres.2014.06.031.
[8] M. Pauly, K. Keegstra, Biosynthesis of the plant cell wall matrix polysaccharide xyloglucan, Annu. Rev. Plant Biol. 67 (2016) 235–259, https://doi.org/10.1146/annurev-arplant-043015-112222.
[9] A. Schultink, L. Liu, L. Zhu, M. Pauly, Structural diversity and function of xyloglucan sidechain substituents, Plants 3 (2014) 526–542, https://doi.org/10.3390/plants3040526.
[10] P. Dutta, S. Giri, T.K. Giri, Xyloglucan as green renewable biopolymer used in drug delivery and tissue engineering, Int. J. Biol. Macromol. 160 (2020) 55–68, https://doi.org/10.1016/j.ijbiomac.2020.05.148.
[11] K. Yamatoya, M. Shirakawa, Xyloglucan: structure, rheological properties, biological functions and enzymatic modification, Curr. Trends Polym. Sci. 8 (2003) 27–72.
[12] K. Yamatoya, K. Yamazaki, M. Shirakawa, O. Baba, Effects of xyloglucan with the partial removal of galactose on plasma lipid concentration, J. Funct.Foods 3 (2011) 275–279, https://doi.org/10.1016/j.jff.2011.05.002.
[13] H. Chen, X. Jiang, S. Li, W. Qin, Z. Huang, Y. Luo, H. Li, D. Wu, Q. Zhang, Y. Zhao, B. Yu, C. Li, D. Chen, Possible beneficial effects of xyloglucan from its degradation by gut microbiota, Trends Food Sci. Technol. 97 (2020) 65–75, https://doi.org/10.1016/j.tifs.2020.01.001.
[14] X. Li, Y. Chen, L. Song, J. Wang, Z. Song, X. Zhao, C. Zhou, Y. Wu, Partial enzymolysis affects the digestion of tamarind seed polysaccharides *in vitro*: degradation accelerates and gut microbiota regulates, Int. J. Biol. Macromol. 237 (2023) 124175, https://doi.org/10.1016/j.ijbiomac.2023.124175.
[15] Y. Kato, J. Uchida, S. Ito, Y. Mitsuishi, Structural analysis of the oligosaccharide units of xyloglucan and their effects on growth of COLO 201 human tumor cells, Int. Congr. Ser. 1223 (2001) 161–164, https://doi.org/10.1016/S0531-5131(01)00413-7.
[16] C.-H. Zhu, Y.-X. Li, Y.-C. Xu, N.-N. Wang, Q.-J. Yan, Z.-Q. Jiang, Tamarind xyloglucan oligosaccharides attenuate metabolic disorders via the gut–liver axis in mice with high-fat-diet-induced obesity, Foods 12 (2023) 1382, https://doi.org/10.3390/foods12071382.
[17] S. Tang, T. Wang, C. Huang, C. Lai, Y. Fan, Q. Yong, Arabinogalactans from Larix principis-rupprechtii: an investigation into the structure-function contribution of side-chain structures, Carbohydr. Polym. 227 (2020) 115354, https://doi.org/10.1016/j.carbpol.2019.115354.
[18] M. Shirakawa, K. Yamatoya, K. Nishinari, Tailoring of xyloglucan properties using an enzyme, Food Hydrocolloids 12 (1998) 25–28, https://doi.org/10.1016/S0268-005X(98)00052-6.
[19] S. Yanmanaka, Y. Yuguchi, H. Urakawa, K. Kajiwara, M. Shirakawa, K. Yamatoya, Gelation of enzymatically degraded xyloglucan extracted from tamarind seed, Sen'i Gakkaishi 55 (1999) 528–532.
[20] Y. Tao, L. Yang, C. Lai, C. Huang, X. Li, Q. Yong, A facile quantitative characterization method of incomplete degradation products of galactomannan by ethanol fractional precipitation, Carbohydr. Polym. 250 (2020) 116951, https://doi.org/10.1016/j.carbpol.2020.116951.
[21] Y. Yan, M. Takemasa, C. Zhao, L. Yu, K. Nishinari, Structure-gelation research on gallate analogs and xyloglucan by rheology, thermal analysis and NMR, Food Hydrocolloids 52 (2016) 447–459, https://doi.org/10.1016/j.foodhyd.2015.07.012.
[22] W.S. York, L.K. Harvey, R. Guillen, P. Albersheim, A.G. Darvill, Structural analysis of tamarind seed xyloglucan oligosaccharides using β-galactosidase digestion and spectroscopic methods, Carbohydr. Res. 248 (1993) 285–301.
[23] M. Zhou, Y. Tao, T. Wang, R. Wang, Q. Yong, Assessing the *in vitro* digestion of Sesbania gum, a galactomannan from S. cannabina, and subsequent impact on the fecal microbiota, J. Funct.Foods 87 (2021) 104766, https://doi.org/10.1016/j.jff.2021.104766.
[24] X. Li, Y. Ren, G. Huang, R. Zhang, Y. Zhang, W. Zhu, K. Yu, Succinate communicates pro-inflammatory signals to the host and regulates bile acid enterohepatic metabolism in a pig model, Food Funct. 13 (2022) 11070–11082, https://doi.org/10.1039/D2FO01958B.
[25] Q. Zhang, D. Zhong, R. Sun, Y. Zhang, R.B. Pegg, G. Zhong, Prevention of loperamide induced constipation in mice by KGM and the mechanisms of different gastrointestinal tract microbiota regulation, Carbohydr. Polym. 256 (2021) 117418, https://doi.org/10.1016/j.carbpol.2020.117418.

[26] J. Liu, X. Chai, T. Guo, J. Wu, P. Yang, Y. Luo, H. Zhao, W. Zhao, O. Nkechi, J. Dong, J. Bai, Q. Lin, Disruption of the ergosterol biosynthetic pathway results in increased membrane permeability, causing overproduction and secretion of extracellular *Monascus* pigments in submerged fermentation, J. Agric. Food Chem. 67 (2019) 13673–13683, https://doi.org/10.1021/acs.jafc.9b05872.
[27] T. Xia, W. Duan, Z. Zhang, S. Li, Y. Zhao, B. Geng, Y. Zheng, J. Yu, M. Wang, Polyphenol-rich vinegar extract regulates intestinal microbiota and immunity and prevents alcohol-induced inflammation in mice, Food Res. Int. 140 (2021) 110064, https://doi.org/10.1016/j.foodres.2020.110064.
[28] M. Han, Y. Liu, F. Zhang, D. Sun, J. Jiang, Effect of galactose side-chain on the self-assembly of xyloglucan macromolecule, Carbohydr. Polym. 246 (2020) 116577, https://doi.org/10.1016/j.carbpol.2020.116577.
[29] J.M. Eklöf, M.C. Ruda, H. Brumer, Distinguishing xyloglucanase activity in endo-β(1→4)glucanases, in: Methods Enzymol, Elsevier, 2012, pp. 97–120, https://doi.org/10.1016/B978-0-12-415931-0.00006-9.
[30] L.A.B.D.C. Carneiro, J. Wurman, P. Dupree, R.J. Ward, The glycoside hydrolase Family 35 β-galactosidase from Trichoderma reesei debranches xyloglucan oligosaccharides from tamarind and jatobá, Biochimie 211 (2023) 16–24, https://doi.org/10.1016/j.biochi.2023.02.009.
[31] S. Zhang, Z. Lin, D. Wang, X. Xu, C. Song, L. Sun, K.H. Mayo, Z. Zhao, Y. Zhou, Galactofuranose side chains in galactomannans from Penicillium spp. modulate galectin-8-mediated bioactivity, Carbohydr. Polym. 292 (2022) 119677, https://doi.org/10.1016/j.carbpol.2022.119677.
[32] X. Zhang, L. Wang, F. Xie, A. Yaseen, B. Chen, G. Zhang, M. Wang, X. Shen, F. Li, A polysaccharide TKP-2-1 from tamarindus indica L: purification, structural characterization and immunomodulating activity, J. Funct.Foods 78 (2021) 104384, https://doi.org/10.1016/j.jff.2021.104384.
[33] Y.P. Silva, A. Bernardi, R.L. Frozza, The role of shortchain fatty acids from gut microbiota in gut-brain communication, Front. Endocrinol. 11 (2020) 25, https://doi.org/10.3389/fendo.2020.00025.
[34] J. Deng, X. Zou, Y. Liang, J. Zhong, K. Zhou, J. Zhang, M. Zhang, Z. Wang, Y. Sun, M. Li, Hypoglycemic effects of different molecular weight konjac glucomannans via intestinal microbiota and SCFAs mediated mechanism, Int. J. Biol. Macromol. 234 (2023) 122941, https://doi.org/10.1016/j.ijbiomac.2022.12.160.
[35] X. Li, R. Guo, X. Wu, X. Liu, L. Ai, Y. Sheng, Z. Song, Y. Wu, Dynamic digestion of tamarind seed polysaccharide: indigestibility in gastrointestinal simulations and gut microbiota changes *in vitro*, Carbohydr. Polym. 239 (2020) 116194, https://doi.org/10.1016/j.carbpol.2020.116194.
[36] A. Koh, F. De Vadder, P. Kovatcheva-Datchary, F. Bäckhed, From dietary fiber to host physiology:short-chain fatty acids as key bacterial metabolites, Cell 165 (2016) 1332–1345, https://doi.org/10.1016/j.cell.2016.05.041.
[37] F.E. Rey, J.J. Faith, J. Bain, M.J. Muehlbauer, R.D. Stevens, C.B. Newgard, J.I. Gordon, Dissecting the *in vivo* metabolic potential of two humangut acetogens, J. Biol. Chem. 285 (2010) 22082–22090, https://doi.org/10.1074/jbc.M110.117713.
[38] N. Reichardt, S.H. Duncan, P. Young, A. Belenguer, C. McWilliam Leitch, K.P. Scott, H.J. Flint, P. Louis, Phylogenetic distribution of three pathways for propionate production within the human gut microbiota, ISME J. 8 (2014) 1323–1335, https://doi.org/10.1038/ismej.2014.14.
[39] P. Louis, P. Young, G. Holtrop, H.J. Flint, Diversity of human colonic butyrate-producing bacteria revealed by analysis of the butyryl-CoA:acetate CoA-transferase gene, Environ. Microbiol. 12 (2010) 304–314, https://doi.org/10.1111/j.1462-2920.2009.02066.x.
[40] H. Huang, J. Chen, Y. Chen, J. Xie, P. Xue, T. Ao, X. Chang, X. Hu, Q. Yu, Metabonomics combined with 16S rRNA sequencing to elucidate the hypoglycemic effect of dietary fiber from tea residues, Food Res. Int. 155 (2022) 111122, https://doi.org/10.1016/j.foodres.2022.111122.
[41] L. Xu, Q. Yu, L. Ma, T. Su, D. Zhang, D. Yao, Z. Li, *In vitro* simulated fecal fermentation of mixed grains on short-chain fatty acid generation and its metabolized mechanism, Food Res. Int. 170 (2023) 112949, https://doi.org/10.1016/j.foodres.2023.112949.
[42] J.-Y. Jiao, L. Fu, Z.-S. Hua, L. Liu, N. Salam, P.-F. Liu, A.-P. Lv, G. Wu, W.-D. Xian, Q. Zhu, E.-M. Zhou, B.-Z. Fang, A. Oren, B.P. Hedlund, H.-C. Jiang, R. Knight, L. Cheng, W.-J. Li, Insight into the function and evolution of the wood–Ljungdahl pathway in *Actinobacteria*, ISME J. 15 (2021) 3005–3018, https://doi.org/10.1038/s41396-021-00935-9.
[43] D. Yao, M. Wu, Y. Dong, L. Ma, X. Wang, L. Xu, Q. Yu, X. Zheng, *In vitro* fermentation of fructooligosaccharide and galactooligosaccharide and their effects on gut microbiota and SCFAs in infants, J. Funct.Foods 99 (2022) 105329, https://doi.org/10.1016/j.jff.2022.105329.
[44] C. Yu, S. Ahmadi, S. Shen, D. Wu, H. Xiao, T. Ding, D. Liu, X. Ye, S. Chen, Structure and fermentation characteristics of five polysaccharides sequentially extracted from sugar beet pulp by different methods, Food Hydrocolloids 126 (2022) 107462, https://doi.org/10.1016/j.foodhyd.2021.107462.
[45] S. Rakoff-Nahoum, M.J. Coyne, L.E. Comstock, An ecological network of polysaccharide utilization among human intestinal symbionts, Curr. Biol. 24 (2014) 40–49, https://doi.org/10.1016/j.cub.2013.10.077.
[46] A. Klindworth, E. Pruesse, T. Schweer, J. Peplies, C. Quast, M. Horn, F.O. Glöckner, Evaluation of general 16S ribosomal RNA gene PCR primers for classical and next-generation sequencing-based diversity studies, Nucleic Acids Res. 41 (2013) e1, https://doi.org/10.1093/nar/gks808, e1.
[47] S.K. Shahi, S.N. Freedman, A.K. Mangalam, Gut microbiome in multiple sclerosis: the players involved and the roles they play, Gut Microb. 8 (2017) 607–615, https://doi.org/10.1080/19490976.2017.1349041.
[48] D. Ndeh, H.J. Gilbert, Biochemistry of complex glycan depolymerisation by the human gut microbiota, FEMS Microbiol. Rev. 42 (2018) 146–164, https://doi.org/10.1093/femsre/fuy002.
[49] G. Déjean, A.S. Tauzin, S.W. Bennett, A.L. Creagh, H. Brumer, Adaptation of syntenic xyloglucan utilization loci of human gut *Bacteroidetes* to polysaccharide side chain diversity, Appl. Environ. Microbiol. 85 (2019) e01491, https://doi.org/10.1128/AEM.01491-19, 19.
[50] D. Di Gioia, I. Aloisio, G. Mazzola, B. Biavati, Bifidobacteria: their impact on gut microbiota composition and their applications as probiotics in infants, Appl. Microbiol. Biotechnol. 98 (2014) 563–577, https://doi.org/10.1007/s00253-013-5405-9.
[51] A.C.M. Leódido, L.E.C. Costa, T.S.L. Araújo, D.S. Costa, N.A. Sousa, L.K.M. Souza, F.B.M. Sousa, M.D.S. Filho, D.F.P. Vasconcelos, F.R.P. Silva, K.M. Nogueira, A. R. Araújo, F.C.N. Barros, A.L.P. Freitas, J.V.R. Medeiros, Anti-diarrhoeal therapeutic potential and safety assessment of sulphated polysaccharide fraction from Gracilaria intermedia seaweed in mice, Int. J. Biol. Macromol. 97 (2017) 34–45, https://doi.org/10.1016/j.ijbiomac.2017.01.006.
[52] B. Yan, C. Huang, C. Lai, Z. Ling, Q. Yong, Production of prebiotic xylooligosaccharides from industrial-derived xylan residue by organic acid treatment, Carbohydr. Polym. 292 (2022) 119641, https://doi.org/10.1016/j.carbpol.2022.119641.
[53] X. Zhao, Q. Wang, T. Wang, Y. Su, C. Huang, C. Lai, Q. Yong, Evaluation of prebiotic ability of xylo-oligosaccharide fractions with different polymerization degrees from bamboo shoot shells, Food Bioprod. Process. 143 (2024) 202–211, https://doi.org/10.1016/j.fbp.2023.11.007.
[54] K. Tamura, G. Dejean, F. Van Petegem, H. Brumer, Distinct protein architectures mediate species-specific beta-glucan binding and metabolism in the human gut microbiota, J. Biol. Chem. 296 (2021) 100415, https://doi.org/10.1016/j.jbc.2021.100415.
[55] Z. Hao, X. Wang, H. Yang, T. Tu, J. Zhang, H. Luo, H. Huang, X. Su, PUL-mediated plant cell wall polysaccharide utilization in the gut Bacteroidetes, Int. J. Mol. Sci. 22 (2021) 3077, https://doi.org/10.3390/ijms22063077.
[56] E.C. Martens, E.C. Lowe, H. Chiang, N.A. Pudlo, M. Wu, N.P. McNulty, D.W. Abbott, B. Henrissat, H.J. Gilbert, D.N. Bolam, J.I. Gordon, Recognition and degradation of plant cell wall polysaccharides by two human gut symbionts, PLoS Biol. 9 (2011) e1001221, https://doi.org/10.1371/journal.pbio.1001221.
[57] D. Zhang, J. Liu, H. Cheng, H. Wang, Y. Tan, W. Feng, C. Peng, Interactions between polysaccharides and gut microbiota: a metabolomic and microbial review, Food Res. Int. 160 (2022) 111653, https://doi.org/10.1016/j.foodres.2022.111653.
[58] X. Cong, X. Sun, J. Qi, H. Li, W. Chai, Q. Zhang, H. Wang, X. Kong, J. Song, L. Pang, M. Jin, D. Li, M. Tan, Z. Duan, GII.13/21 Noroviruses recognize glycans with a terminal β-galactose via an unconventional glycan binding site, J. Virol. 93 (2019) e00723, https://doi.org/10.1128/JVI.00723-19, 19.
[59] R. Pujari, G. Banerjee, Impact of prebiotics on immune response: from the bench to the clinic, Immunol. Cell Biol. 99 (2021) 255–273, https://doi.org/10.1111/imcb.12409.
[60] N. Singh, A. Gurav, S. Sivaprakasam, E. Brady, R. Padia, H. Shi, M. Thangaraju, P.D. Prasad, S. Manicassamy, D.H. Munn, J.R. Lee, S. Offermanns, V. Ganapathy, Activation of Gpr109a, Receptor for niacin and the commensal metabolite butyrate, suppresses colonic inflammation and carcinogenesis, Immunity 40 (2014) 128–139, https://doi.org/10.1016/j.immuni.2013.12.007.